



HAL
open science

IDH mutation status in a series of 88 head and neck chondrosarcomas: different profile between tumors of the skull base and tumors involving the facial skeleton and the laryngotracheal tract

Matthias Tallegas, Elodie Miquelstorena-Standley, Corinne Labit-Bouvier, Cécile Badoual, Arnaud François, Anne Gomez-Brouchet, Sébastien Aubert, Christine Collin, Anne Tallet, Gonzague de Pinieux

► **To cite this version:**

Matthias Tallegas, Elodie Miquelstorena-Standley, Corinne Labit-Bouvier, Cécile Badoual, Arnaud François, et al.. IDH mutation status in a series of 88 head and neck chondrosarcomas: different profile between tumors of the skull base and tumors involving the facial skeleton and the laryngotracheal tract. *Human Pathology*, 2019, 84, pp.183-191. 10.1016/j.humpath.2018.09.015 . hal-02316608

HAL Id: hal-02316608

<https://normandie-univ.hal.science/hal-02316608>

Submitted on 21 Oct 2021

HAL is a multi-disciplinary open access archive for the deposit and dissemination of scientific research documents, whether they are published or not. The documents may come from teaching and research institutions in France or abroad, or from public or private research centers.

L'archive ouverte pluridisciplinaire **HAL**, est destinée au dépôt et à la diffusion de documents scientifiques de niveau recherche, publiés ou non, émanant des établissements d'enseignement et de recherche français ou étrangers, des laboratoires publics ou privés.



Distributed under a Creative Commons Attribution - NonCommercial 4.0 International License

IDH Mutation Status in a Series of 88 Head and Neck Chondrosarcomas: Different Profile Between Tumors of the Skull Base and Tumors Involving the Facial Skeleton and the Laryngotracheal Tract

Matthias TALLEGAS, MD¹, Élodie MIQUELESTORENA-STANDLEY, MD^{1,9}, Corinne LABIT-BOUVIER, MD, PhD², Cécile BADOUAL, MD, PhD^{3,4}, Arnaud FRANCOIS, MD⁵, Anne GOMEZ-BROUCHET, MD, PhD⁶, Sébastien AUBERT, MD, PhD⁷, Christine COLLIN, PhD⁸, Anne TALLET, PharmD⁸, Gonzague de PINIEUX MD, PhD^{1,9,10}

1: CHRU de Tours, Service d'Anatomie et Cytologie Pathologiques, Tours, France.

2: CHU de Marseille, Service d'Anatomie et Cytologie Pathologiques, Marseille, France.

3: Hôpital Européen Georges Pompidou, Service d'Anatomie Pathologique, APHP, Paris, France.

4: Université Paris Descartes, Sorbonne Paris-Cité, Paris, France.

5: CHU de Rouen, Service d'Anatomie et Cytologie Pathologiques, Rouen, France.

6: CHU de Toulouse, Service d'Anatomie et Cytologie Pathologiques, Toulouse, France.

7: CHU de Lille, Service d'Anatomie et Cytologie Pathologiques, Lille, France.

8: CHRU de Tours, Plateforme de Génétique Moléculaire des Cancers, Tours, France.

9: Université François Rabelais, Faculté de Médecine, Tours, France.

10: Laboratoire d'étude des sarcomes osseux et remodelage des tissus calcifiés, PhyOS - INSERM UMR 1238, Faculté de Médecine de Nantes, Université de Nantes, 44034 Nantes cedex 1, France.

Running title: *IDH* Mutations in Head and Neck Chondrosarcomas

The authors declare not having received any specific funding.

Corresponding author:

Professor Gonzague de PINIEUX

Service d'Anatomie et Cytologie Pathologiques-Hôpital Trousseau-CHRU de Tours-37044 Tours Cedex 9, France.

depinieux@med.univ-tours.fr

Abstract

Chondrosarcomas are rare primary malignant bone tumors that involve the head and neck region in 1% to 12% of cases. Central conventional chondrosarcoma is the most common subtype and is associated with isocitrate dehydrogenase 1 and 2 (*IDH1* and *IDH2*) gene mutations in 50% to 60% of cases. We aimed to define the frequency of *IDH1* and *IDH2* gene mutations in a multicenter series of 88 cases of chondrosarcoma of the head and neck, including tumors involving the base of the skull (n=30), the facial skeleton (n=11), and the laryngeal and tracheal cartilages (n=47). Petrous bone and cricoid cartilage were the most frequently involved sites for chondrosarcomas of the skull base and laryngotracheal tract (respectively 43.3% and 31.9%). Overall, 64.9% of craniofacial chondrosarcomas featured *IDH* mutations, with a high rate for skull-base tumors (85.7%) but no *IDH* mutations in tumors of the facial skeleton. This different mutational profile could be related to the type of ossification, the bones of the base of the skull mainly resulting from endochondral ossification and those of the face from intramembranous ossification. Conversely, mutation was infrequent in chondrosarcomas involving the laryngeal and tracheal cartilages (11.8% of 47 cases). Evaluation of *IDH* mutation status may be a useful diagnostic tool for bone tumors of the skull base, which are most often assessable with only small biopsy samples. The low rate of *IDH* mutations observed in laryngotracheal chondrosarcomas suggests a different mode of tumorigenesis needing further exploration.

1. Introduction

Chondrosarcomas are rare tumors, with an incidence estimated between 0.1 and 0.3 cases per 100,000 people. They represent the second most frequent primitive malignant bone sarcoma after osteosarcomas. They mainly affect adults older than 40 years of age and most commonly involve the pelvis, femur, humerus and ribs [1–3]. Localization in the head and neck region is rarer, occurring in 1% to 12% of cases [4,5]. The current model of oncogenesis of central and periosteal conventional cartilaginous tumors is characterized by early alterations of the isocitrate dehydrogenase 1 (*IDH1*) and isocitrate dehydrogenase 2 (*IDH2*) genes [6]. These mutations were initially described in 2011 in cartilaginous tumors of patients with enchondromatosis, who are also more likely to develop other tumors such as gliomas and acute myeloid leukemia. At that time, gliomas were already known to harbor *IDH* gene mutations (as observed in 80% of diffuse gliomas and secondary glioblastomas[7–9]). A high rate of 87% to 90% of *IDH1* mutations was found in cartilaginous tumors of patients with Ollier’s disease and Maffucci syndrome [10,11]. The incidence of these mutations was then evaluated in sporadic conventional central and periosteal tumors of appendicular and axial skeleton, with 52% of *IDH* gene mutations in low-grade central cartilaginous tumors (enchondromas or grade 1 chondrosarcomas) and 58.9% of central high-grade chondrosarcomas, most of them (88%) involving *IDH1* [12]. Acral tumors showed a high mutation rate (90%) whereas tumors involving the long bones of the appendicular skeleton and the flat bones showed a lower *IDH* mutation rate (respectively 53% and 35%). These abnormalities were also found in periosteal cartilaginous tumors (71% of periosteal chondromas and 15% to 100% of periosteal chondrosarcomas [12,13]). *IDH* mutations are dominant and involve the exon 4 of the gene, which leads to the substitution of an amino-acid on the active site of the protein. According to Amary *et al.*, the most frequent mutation (39.5%) is an R132C transition (CGT>TGT). The other mutations mainly include R132G (CGT>GGT) transversions in 19.7% of cases, R132L (CGT>CTT) in 7.4% and R132S (CGT>AGT) in 7.4%. A few *IDH2* mutations (8.6%) are also found, most of them being a R172S transversion (AGG>AGT) and more rarely R140 [12]. *IDH* mutations have no prognostic impact in chondrosarcoma and are not found in other mesenchymal tumors, especially in osteosarcoma and in other cartilaginous tumors such as chondroblastoma, chondromyxoid fibroma, and peripheral, mesenchymal and clear cell chondrosarcomas.

The discovery of *IDH* gene mutations in conventional central cartilaginous tumors is a valuable molecular tool for the differential diagnosis of these tumors and has gained particular interest since the introduction of several clinical trials targeting *IDH* mutated proteins in various tumors

including chondrosarcoma, for which classical chemotherapy and radiotherapy have shown limited efficiency in the treatment of advanced high-grade tumors.

The few studies focusing on skull base chondrosarcomas have reported an *IDH1* mutation rate of 46.1% to 71.4% [14,15]. The *IDH* mutational status of chondrosarcomas arising from the cartilaginous structures of the upper respiratory tract has, to the best of our knowledge, not been evaluated so far. The aim of this study was to evaluate the *IDH* mutation status in a series of 88 chondrosarcomas of the head and neck region, including 47 tumors of the laryngotracheal tract and 41 craniofacial tumors.

2. Materials and Methods

2.1. Selection of patients

This retrospective multicenter French study meets the requirements for the use of biological material proposed by institutional ethics guidelines. All tumors included in this study were chondrosarcomas diagnosed in five centers of the French Bone Pathology Group network RESOS (Lille, Marseille, Rouen, Toulouse and Tours) and an ORL pathology expert center (European Hospital Georges Pompidou) between 2000 and 2018 and involved the laryngotracheal cartilages and the craniofacial skeleton. All cases causing differential diagnosis issues were reviewed collegially by a quorum of bone pathologists, who had access to the clinical and radiological elements of the patient's chart.

We collected 103 samples (50 surgical specimens, 40 biopsies, and 13 samples of unspecified type) from 88 patients. Among these 88 cases of chondrosarcoma, 47 involved the laryngotracheal cartilages and 41 the cranio-facial skeleton (including the skull base and facial skeleton). The slides and paraffin blocks were centralized at the University Hospital of Tours (France).

All tumors with available slides, stained by hematoxylin-eosin-saffron, were reviewed by two pathologists (GdP and MT). WHO criteria for grading chondrosarcomas were applied, even if they have not been validated for the skull base, facial skeleton and laryngotracheal locations [16–18].

2.2. Genotyping analysis

2.2.1. DNA extraction

Genomic DNA (gDNA) was extracted from formalin-fixed paraffin-embedded (FFPE) samples (decalcification data not available). gDNA was isolated from tissue samples by using a Maxwell 16 Instrument (Promega) with the Maxwell 16 FFPE Plus LEV DNA purification kit (Promega) according to the manufacturer's instructions.

2.2.2. Pyrosequencing

We focused on substitutions at the R132 codon of the *IDH1* gene (loci c.394 and c.395) and the R172 codon of *IDH2* gene (loci c.515 and c.516).

PCR was performed using PyroMark PCR Kit (Qiagen): 30 ng DNA was added to 20 μ l of a reaction mix containing 2.5 μ l CoralLoad 10x, 12.5 μ l master mix, 3 μ l H₂O and 10 pmol each primer. The PCR conditions were 15 min at 95°C followed by 20 sec at 94°C, 30 sec at 53°C and 20 sec at 72°C for 42 cycles, and 5 min at 72°C.

An amount of 10 μ l PCR product was added to a DNA immobilization mix containing 1 μ l streptavidin beads (GE Healthcare), 40 μ l PyroMark binding buffer (Qiagen) and 29 μ l H₂O on a 24-well plate. After sealing, the plate was vortexed for 5 to 10 min at 1400 rpm on a plate-mixer. With a PyroMark workstation, single stranded DNA was added to a PyroMark Q24 plate in 25 μ l (8 pmol) sequencing primer (Table 1) in an annealing buffer. After 2 min at 80°C, the plate was kept at room temperature for 20 min before processing the pyrosequencing reaction.

Pyrosequencing involved use of PyroMark Gold Q24 reagents (Qiagen) on a PyroMark Q24 (Qiagen). The sequences analyzed were GACGACCTA for *IDH1* and GCAGGCACG for *IDH2*. The nucleotide dispensation order was CGTACTAGACTA for *IDH1* and CGCTACTGTACAC for *IDH2* (Table 1). Results were analyzed using PyroMark sw 2.0.6 software (Qiagen).

2.2.3. PCR amplification and direct sequencing reaction

Samples defined as mutated by pyrosequencing underwent direct sequencing (Sanger sequencing, i.e. the reference method) to validate the results. We also tested negative cases. The analysis concerned exon 4 of *IDH1* and exon 4 of *IDH2*.

For PCR reaction, 2 μ l polymerase buffer 10x, 1.2 μ l of 25 mM of MgCl₂, 0.4 μ l of 10 mM dNTP, 1 μ l each 10 μ M primer, 1 unit of AmpliTaq Gold DNA Polymerase (Applied Biosystems), 12 μ l H₂O and 80 ng gDNA were mixed in a final volume of 20 μ l. PCR conditions were 8 min at 95°C followed by 45 sec at 94°C, 45 sec at 55°C and 1 min at 72°C, for 35 cycles and a final elongation for 7 min at 72°C.

PCR products were purified with ExoI and Fast-AP (ThermoScientific) according to the manufacturer's instructions. The sequencing reaction was performed using Big Dye terminator V3.1 cycle sequencing kit (Applied Biosystems) according to the manufacturer's protocol, and 2 μ M primers. The sequencing products were purified by using the Big Dye Xterminator purification kit (Applied Biosystems) before running on a 3130 Genetic Analyzer (Applied Biosystems). The sequencing data were analyzed by using Sequencing Analysis software (Applied Biosystems). The sequencing profile was not interpretable for 17/88 cases (19.3%) due to unsuitable genetic material.

2.3. Statistical analysis

Statistical analysis involved use of GraphPad Prism 5 for Windows (GraphPad Software. La Jolla, CA, USA). We compared patients with a skull-base chondrosarcoma to those with a chondrosarcoma involving the facial skeleton and those with a chondrosarcoma of the larynx and trachea. Continuous variables were compared using Mann-Whitney test, categorical variables using Fisher's exact test. $P < 0.05$ was considered significant.

3. Results

3.1. Clinical and histological features

The clinical and histological data of the two groups of tumors (tumors involving the laryngo-tracheal tract and tumors involving the craniofacial skeleton) are summarized in Tables 2 and 3 respectively.

All bone tumors showed morphological features consistent with the diagnosis of chondrosarcoma. Tumors arising from cartilaginous structures showed at least an increased cellularity, various degrees of nuclear atypia and signs of interstitial chondrocytic proliferation including formation of isogenic islands and binucleations. An invasion of adjacent normal cartilaginous structures or of osseous metaplastic structures was also observed in a subset of cases (Fig. 1A and 1B).

Tumors were mainly grade 1 for chondrosarcomas of the laryngotracheal tract (58.7%) and grade 2 for chondrosarcomas of the craniofacial skeleton (70.3%) (Fig. 1C).

3.2. *IDH* mutation status

3.2.1. Tumors of the laryngotracheal tract

Molecular analysis of *IDH* mutational status could be performed for 34/47 cases (72.3%): 4 (11.8%) showed an *IDH1* mutation — R132C in 3 cases and R132G in 1 case. No *IDH2* mutation could be detected (Table 4).

3.2.2. Tumors of the craniofacial skeleton

A molecular analysis could be performed for 37/41 tumors (90.2%), with an *IDH1* mutation observed in 24/37 cases (64.9%). Separating the tumors from the skull base and facial bones, the *IDH1* mutation rate was respectively 85.7% (24/28) and 0% (0/9). Mutations were R132C substitution in 15/24 cases (62.5%), R132G in 4/24 (16.7%), R132L in 3/24 (12.5%), R132S in 1/24 (4.2%) and R132H in 1/24 (4.2%). No *IDH2* mutation could be detected (Table 5).

3.3. Comparison of *IDH* mutation status depending on anatomic location

Analysis of *IDH* mutational status could be performed for 34/47 tumors (72.3%) involving the laryngotracheal tract, a lower rate than for those involving the skull base (93.3%, $p = 0.0367$). Finally, frequency of *IDH1* mutations was significantly lower in chondrosarcomas of the maxillofacial skeleton (0%, $p = 5.7 \cdot 10^{-6}$) and laryngotracheal tract (11.8%, $p = 3.2 \cdot 10^{-9}$) than in skull-based tumors.

4. Discussion

This multicenter study is, to our knowledge, the first to focus on *IDH1* and *IDH2* mutations in chondrosarcomas of the head and neck region as a whole, and more specifically on tumors involving the laryngotracheal tract.

Among the 47 tumors involving the laryngotracheal cartilages, tumors preferentially involved the larynx (85.7%) and mainly the cricoid cartilage, in accordance with previous data [16,17,19]. These chondrosarcomas featured a particularly low rate of *IDH1* mutation (11.8%), which suggests another pathway of tumorigenesis.

We may only argue that the larynx shares with most of the facial bones, where the incidence of *IDH* mutations is here null, a common embryologic origin as they are derived from the pharyngeal arches (PA). Indeed, maxillary and mandibular bones are derived from the 1st PA, the epiglottic and thyroid cartilages from the 4th PA, and the cricoid, arytenoid, corniculate and cuneiform cartilages from the 6th PA. However, the trachea, vomer and nasal cartilages have a distinct embryonic origin, occurring respectively from the laryngotracheal groove (foregut endoderm) and from the frontonasal process (Fig. 2).

Another hypothesis that could also be discussed was that the few laryngotracheal *IDH*-mutated tumors arose in areas of osseous metaplasia. Indeed, although only a few studies focused on secondary ossification of the laryngeal cartilages, it seems to be a common process. In a retrospective study of 359 patients aged 10 to 59 who underwent lateral cephalometric radiography, ossification of the cricoid or thyroid cartilages was found in 17% to 36% of cases [20]. The thyroid cartilage was ossified more often than the cricoid cartilage, and the frequency of ossification increased with age (less than 5% before age 20 to more than 90% after age 60). Furthermore, in an autopsy series of 25 adults between 20 and 87 years old, ossification of the tracheal cartilaginous rings was found in 52% of cases with, again, the frequency increasing with age [21]. In our series, ossified areas could be histologically observed in 14 of the 47 chondrosarcomas of the laryngotracheal tract with available slides (data not shown). Among these tumors, only one featured an *IDH1* mutation. The three other *IDH* mutated chondrosarcomas did not show any ossification, which suggests no relation between the occurrence of osseous metaplasia of cartilaginous structures and *IDH* mutation.

As for the skull base, chondrosarcomas were more often localized in the petrous bone (43.3%), whereas tumors of the facial skeleton mostly involved the maxillary bone (45.5%) and the nasal cartilages (45.5%).

Understanding of embryological development and knowledge of differences in the ossification process of the different parts of the craniofacial skeleton could give keys to the various rates of *IDH1* gene mutation observed in tumors of the base of the skull and facial bones. The craniofacial skeleton is composed of the calvaria (or cranial vault; composed of the upper part of the occipital, parietal and frontal bones), the skull base (composed of the major part of the sphenoid, ethmoid, temporal and the lower part of the occipital bones) and the facial skeleton (composed of an osseous skeleton including the lower part of the frontal bone, the lacrimal, zygomatic and nasal bones, the vomer, the maxillary bone, the medial plates of the sphenoid bone and the mandible) and of the nasal cartilaginous skeleton. Concerning the osseous craniofacial skeleton, the calvaria and the skull base are derived from the neurocranium, which can be subdivided into the desmocranium, corresponding to the bones of the cranial vault, and the chondrocranium, corresponding to the skull base; whereas the facial bones are derived from the viscerocranium (Fig. 3A).

The base of the skull is the cornerstone that joins the cranial vault to the vertebrae and to the facial bones. This unique osseous structure has a dual embryologic origin: the anterior part (rostral to the notochord) is derived from neural crest cells, like the facial bones (viscerocranium),

whereas the posterior part (caudal to the notochord) is derived from the paraxial mesoderm (Fig. 3B). During the 4th week of development, mesenchymal cells of the paraxial mesoderm and neural crest cells condense to form the lower part of the ectomeningeal capsule. The inner layer of this capsule undergoes progressive chondrification between the 7th and 8th weeks of development, which leads to formation of an irregular plate: the chondrocranium. This plate undergoes a progressive endochondral ossification, from caudal to rostral side, from numerous ossification centers. Nevertheless, this ossification remains incomplete as large areas remain cartilaginous throughout the fetal life and persist during the neonatal period. Finally, individual bones of the cranial base are bound by cartilaginous tissue, termed synchondroses, similar in structure to the long-bone growth plate. Unlike the base of the skull, most of the cranial vault bones (desmocranium) undergo an intramembranous ossification (Fig. 3C), without intermediate cartilaginous tissue [22–29].

On the other hand, the facial bones, mainly derived from the neural crest cells of the first branchial arch and frontonasal process, show both endochondral and intramembranous ossification. Actually, the vomer and frontal, maxillary, lacrimal and zygomatic bones undergo an exclusive intramembranous ossification, whereas the mandible undergoes concomitant intramembranous (body) and endochondral ossification (condyle and coronoid) [14,15,30].

In summary, the petrous and sphenoid bones, the two bones most frequently affected by chondrosarcomas in the skull base showing a high *IDH* mutation rate, differ in their embryonic formation because they derive from different precursors. The petrous bone and posterior part of the sphenoid bone belong to the posterior part of the chondrocranium and so derive from the paraxial mesoderm, whereas the anterior part of the sphenoid bone derives from the neural crest cells. Furthermore, the facial bones, with chondrosarcomas showing a low rate of *IDH* mutation, also mainly derive from neural crest cells. Thus, the *IDH* mutation status of craniofacial chondrosarcomas may be independent of the embryonic germ layer at the origin of the tissue. However, this *IDH* mutation status might be linked with the mode of ossification, considering that cartilaginous tumors associated with a high level of *IDH* mutations arise in bones of the base of the skull, mainly formed by endochondral ossification.

This study represents the largest series to date (n=30) evaluating the *IDH* mutation rate in chondrosarcomas of the base of the skull. We found 85.7% of *IDH1* mutated chondrosarcomas in this location, which is higher than reported in smaller previous studies (46.1% to 71.4%) [14,15], and close to what was reported for bones of hand and feet and enchondromatosis [11]. This difference might be related to the technique of pyrosequencing used to detect *IDH*

mutations in this series, which is more sensitive than traditional Sanger sequencing. In our experience, the *IDH* mutation highlighted by pyrosequencing could not be confirmed with Sanger sequencing in a significant subset of cases which were not interpretable. Mutation subtypes observed in skull base chondrosarcomas are similar to those observed in conventional central chondrosarcomas of the extremities, with a predominance of R132C mutations (62.5%).

IDH mutational status assessment can then be a sensitive and specific additional diagnostic tool for small biopsy specimens in chondrosarcomas of the skull base, especially in the differential diagnosis with chordoma and its morphological variants; or more exceptionally, with chondromyxoid fibroma, both tumors showing absence of *IDH* gene mutations [12,14,15,30,31] In conclusion, our series shows that among chondrosarcomas involving the craniofacial skeleton, tumors arising from the skull base harbor a high *IDH1* mutation rate (24/28, 85.7%), but none in tumors arising from the osteo-cartilaginous skeleton of the face (0/9). This difference seems to be related to the type of ossification involved in these different areas, endochondral versus endomembranous. Thus, *IDH* gene mutation search may be a valuable diagnostic tool for detecting chondrosarcomas of the skull base.

In addition, this series puts forward for the first time, to the best of our knowledge, that laryngotracheal chondrosarcomas are associated with a low rate of *IDH* mutations (4/34, 11.8%), independent of the presence of metaplastic ossification foci. Further investigations are needed to explore the mechanisms involved in the tumorigenesis of chondrosarcomas in this localization.

Disclosure/Conflict of interest:

The authors declare no conflict of interest.

References

- [1] Fletcher CD, Bridge JA, Hogendoorn PCW, Mertens F. WHO Classification of Tumours of Soft Tissue and Bone. vol. 5. 4th Edition. Lyon: IARC Press; 2013.
- [2] Valery PC, Laversanne M, Bray F. Bone cancer incidence by morphological subtype: a global assessment. *Cancer Causes Control CCC* 2015;26:1127–39. doi:10.1007/s10552-015-0607-3.
- [3] Giuffrida AY, Burgueno JE, Koniari LG, Gutierrez JC, Duncan R, Scully SP. Chondrosarcoma in the United States (1973 to 2003): an analysis of 2890 cases from the SEER database. *J Bone Joint Surg Am* 2009;91:1063–72. doi:10.2106/JBJS.H.00416.
- [4] Ellis MA, Gerry DR, Byrd JK. Head and neck chondrosarcomas: Analysis of the Surveillance, Epidemiology, and End Results database. *Head Neck* 2016;38:1359–66. doi:10.1002/hed.24434.
- [5] Ruark DS, Schlehaider UK, Shah JP. Chondrosarcomas of the head and neck. *World J Surg* 1992;16:1010–5; discussion 1015-1016.
- [6] Samuel AM, Costa J, Lindskog DM. Genetic alterations in chondrosarcomas – keys to targeted therapies? *Cell Oncol* 2014;37:95–105. doi:10.1007/s13402-014-0166-8.
- [7] Yan H, Parsons DW, Jin G, McLendon R, Rasheed BA, Yuan W, et al. *IDH1* and *IDH2* Mutations in Gliomas. *N Engl J Med* 2009;360:765–73. doi:10.1056/NEJMoa0808710.
- [8] Mondesir J, Willekens C, Touat M, de Botton S. *IDH1* and *IDH2* mutations as novel therapeutic targets: current perspectives. *J Blood Med* 2016;7:171–80. doi:10.2147/JBM.S70716.
- [9] Yang H, Ye D, Guan K-L, Xiong Y. *IDH1* and *IDH2* mutations in tumorigenesis: mechanistic insights and clinical perspectives. *Clin Cancer Res Off J Am Assoc Cancer Res* 2012;18:5562–71. doi:10.1158/1078-0432.CCR-12-1773.
- [10] Pansuriya TC, van Eijk R, d’Adamo P, van Ruler MAJH, Kuijjer ML, Oosting J, et al. Somatic mosaic *IDH1* and *IDH2* mutations are associated with enchondroma and spindle cell hemangioma in Ollier disease and Maffucci syndrome. *Nat Genet* 2011;43:1256–61. doi:10.1038/ng.1004.
- [11] Amary MF, Damato S, Halai D, Eskandarpour M, Berisha F, Bonar F, et al. Ollier disease and Maffucci syndrome are caused by somatic mosaic mutations of *IDH1* and *IDH2*. *Nat Genet* 2011;43:1262–5. doi:10.1038/ng.994.
- [12] Amary MF, Bacsi K, Maggiani F, Damato S, Halai D, Berisha F, et al. *IDH1* and *IDH2* mutations are frequent events in central chondrosarcoma and central and periosteal chondromas but not in other mesenchymal tumours. *J Pathol* 2011;224:334–43. doi:10.1002/path.2913.
- [13] Cleven AHG, Zwartkuis E, Hogendoorn PCW, Kroon HM, Briaire-de Bruijn I, Bovée JVMG. Periosteal chondrosarcoma: a histopathological and molecular analysis of a rare chondrosarcoma subtype. *Histopathology* 2015;67:483–90. doi:10.1111/his.12666.
- [14] Arai M, Nobusawa S, Ikota H, Takemura S, Nakazato Y. Frequent *IDH1/2* mutations in intracranial chondrosarcoma: a possible diagnostic clue for its differentiation from chordoma. *Brain Tumor Pathol* 2012;29:201–6. doi:10.1007/s10014-012-0085-1.
- [15] Kanamori H, Kitamura Y, Kimura T, Yoshida K, Sasaki H. Genetic characterization of skull base chondrosarcomas. *J Neurosurg* 2015;123:1036–41. doi:10.3171/2014.12.JNS142059.
- [16] Thompson LDR, Gannon FH. Chondrosarcoma of the larynx: a clinicopathologic study of 111 cases with a review of the literature. *Am J Surg Pathol* 2002;26:836–51.
- [17] Chin OY, Dubal PM, Sheikh AB, Unsal AA, Park RCW, Baredes S, et al. Laryngeal chondrosarcoma: A systematic review of 592 cases. *The Laryngoscope* 2017;127:430–9. doi:10.1002/lary.26068.

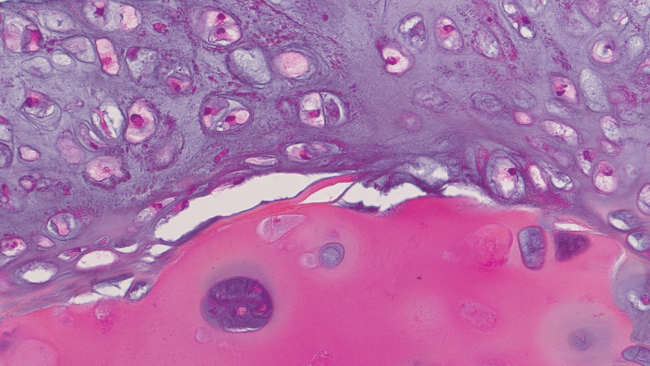
- [18] Bloch OG, Jian BJ, Yang I, Han SJ, Aranda D, Ahn BJ, et al. Cranial Chondrosarcoma and Recurrence. *Skull Base* 2010;20:149–56. doi:10.1055/s-0029-1246218.
- [19] Potochny EM, Huber AR. Laryngeal Chondrosarcoma. *Head Neck Pathol* 2013;8:114–6. doi:10.1007/s12105-013-0483-7.
- [20] Mupparapu M, Vuppalapati A. Ossification of laryngeal cartilages on lateral cephalometric radiographs. *Angle Orthod* 2005;75:196–201.
- [21] Kusafuka K, Yamaguchi A, Kayano T, Takemura T. Ossification of tracheal cartilage in aged humans: a histological and immunohistochemical analysis. *J Bone Miner Metab* 2001;19:168–174.
- [22] Som PM, Curtin HD, Liu K, Mafee MF. Current Embryology of the Temporal Bone, Part I: the Inner Ear. *Neurographics* 2016;6:250–65. doi:10.3174/ng.4160166.
- [23] Som PM, Naidich TP. Development of the Skull Base and Calvarium: An Overview of the Progression from Mesenchyme to Chondrification to Ossification. *Neurographics* 2013;3:169–84. doi:10.3174/ng.4130069.
- [24] Nie X. Cranial base in craniofacial development: Developmental features, influence on facial growth, anomaly, and molecular basis. *Acta Odontol Scand* 2005;63:127–35. doi:10.1080/00016350510019847.
- [25] Sadler TW, Sadler-Redmond SL, Tosney K, Byrne J, Imseis H. *Langman’s medical embryology*. 13th Edition. Baltimore, MD: Lippincott Williams & Wilkins; 2015.
- [26] Evans DJR, Noden DM. Spatial relations between avian craniofacial neural crest and paraxial mesoderm cells. *Dev Dyn Off Publ Am Assoc Anat* 2006;235:1310–25. doi:10.1002/dvdy.20663.
- [27] Sperber GH, Sperber SM, Guttmann GD. *Craniofacial Embryogenetics and Development*. 3rd Edition. Shelton, United States: People’s Medical Publishing House - USA LTD; 2010.
- [28] Blaser SI, Padfield N, Chitayat D, Forrest CR. Skull base development and craniosynostosis. *Pediatr Radiol* 2015;45:485–96. doi:10.1007/s00247-015-3320-1.
- [29] Gilbert SF. *Developmental Biology*. 11th Edition. Sunderland (MA): Sinauer Associates; 2016.
- [30] Kitamura Y, Sasaki H, Yoshida K. Genetic aberrations and molecular biology of skull base chordoma and chondrosarcoma. *Brain Tumor Pathol* 2017;34:78–90. doi:10.1007/s10014-017-0283-y.
- [31] Sa JK, Lee I-H, Hong SD, Kong D-S, Nam D-H. Genomic and transcriptomic characterization of skull base chordoma. *Oncotarget* 2017;8:1321–8. doi:10.18632/oncotarget.13616.

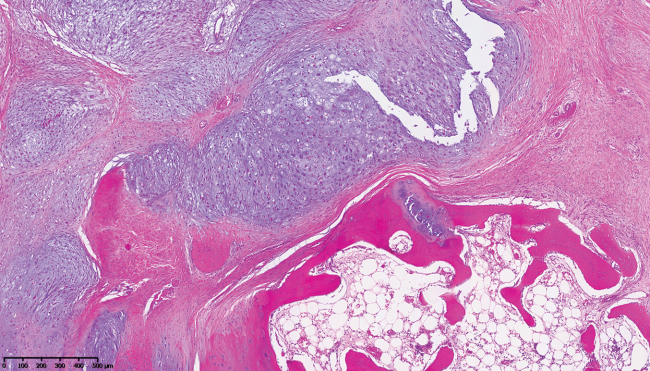
Figure legends

Fig.1. A: Well-differentiated grade 1 chondrosarcoma of the cricoid (H&E staining x400). The tumor cartilage is in contact with the cricoid cartilage. B: Grade 2 chondrosarcoma of the cricoid abutting a focus of osseous metaplasia (H&E staining x50). C: Grade 2 chondrosarcoma of the skull base characterized by large and hypercellular areas of hyaline cartilage containing chondrocytes with plump nuclei of uniform size (H&E staining x200).

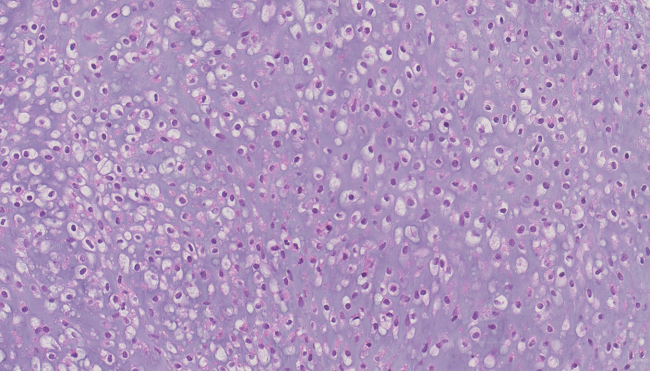
Fig.2. Embryonic origin of the facial skeleton and laryngotracheal cartilages. The nasal skeleton is composed of osseous structures (nasal bones, nasal part of the frontal bone, vomer and perpendicular plate of the ethmoid) and 5 cartilages (septal, greater and lesser alar, lateral and vomeronasal cartilages) and is derived from the nasofrontal process. At the opposite, the maxilla, mandible and laryngotracheal cartilages are derived from pharyngeal arches (the maxilla and mandible from the 1st PA, the hyoid bone from the 2nd and 3rd PA, the epiglottic and thyroid cartilages from the 4th PA and the cricoid cartilage from the 6th PA). The trachea is derived from a ventral depression of the foregut endoderm (laryngotracheal groove).

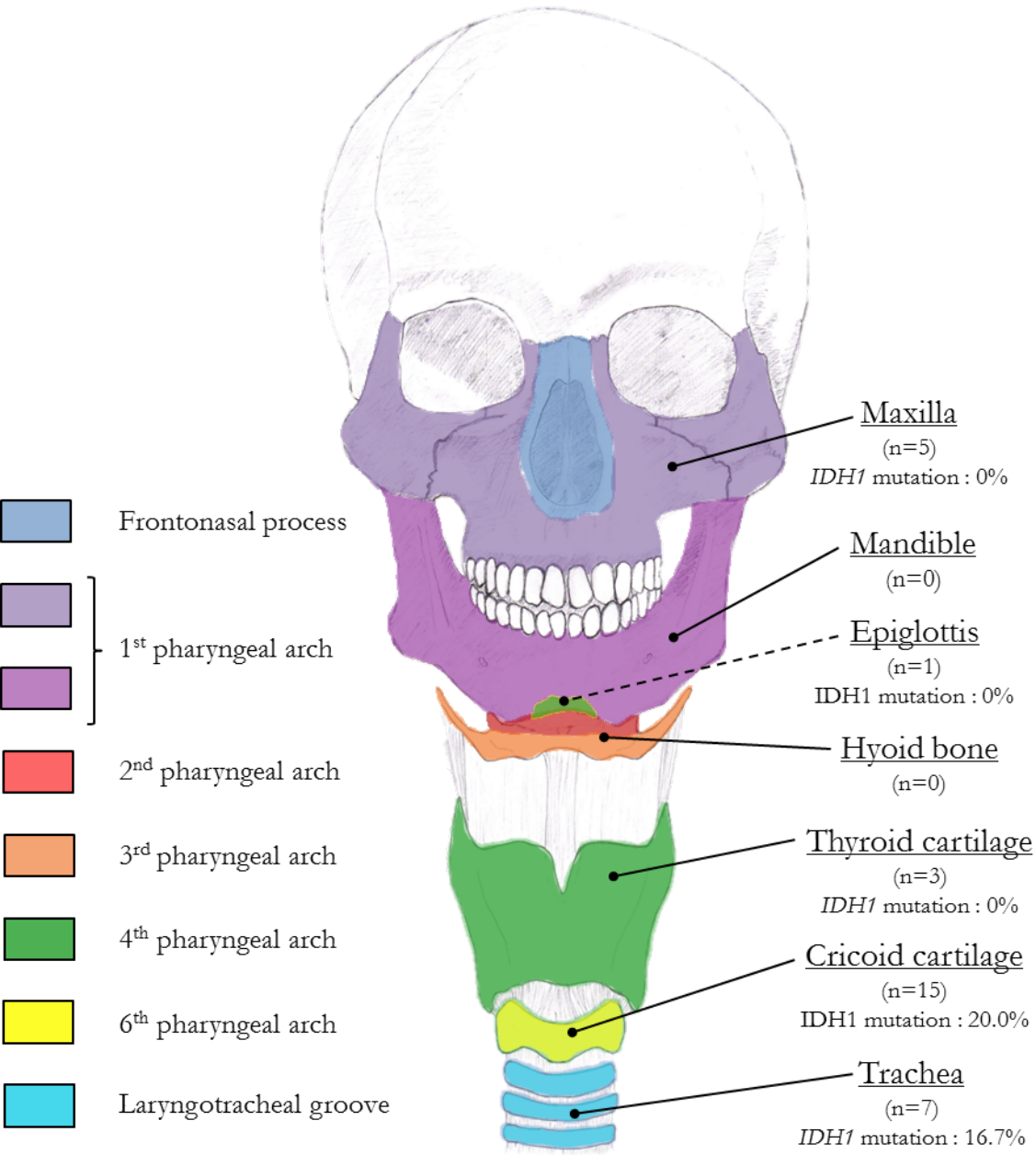
Fig.3. A: Embryonal structures forming the craniofacial skeleton. The neurocranium is divided into the desmocranium (grey), corresponding to the cranial vault; chondrocranium (red), corresponding to the skull base; and viscerocranium (green), corresponding to facial bones. B: Cells of origin of the craniofacial skeleton. The viscerocranium and anterior part of both the chondrocranium and desmocranium (relative to the notochord) are derived from neural crest cells (blue), whereas the posterior part of chondrocranium and desmocranium is derived from the paraxial mesoderm (yellow). C: *IDH* mutation status of the 35 chondrosarcomas involving the skull base and facial skeleton (excluding cases with NOS location) according to the type of ossification (intramembranous ossification in beige; endochondral ossification in purple). The cranial vault and facial bones are mainly formed by intramembranous ossification (with the exception of the coronoid process and condyles of the mandible), whereas the skull base is mainly formed by endochondral ossification, with the exception of the posterior part of the sphenoid bone and of squamous part of the temporal bone.

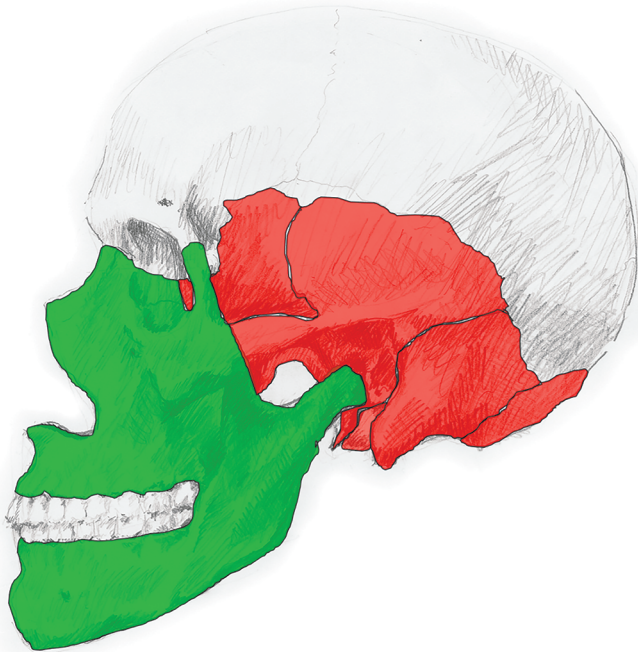


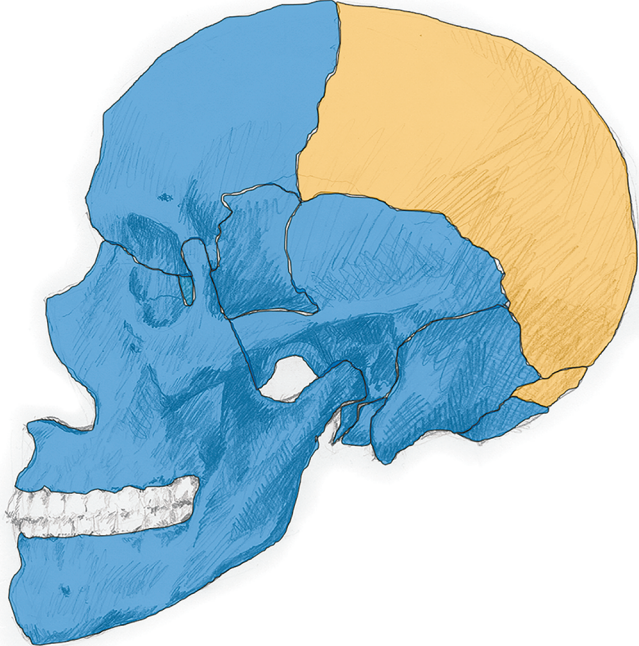


0 100 200 300 400 500 μm









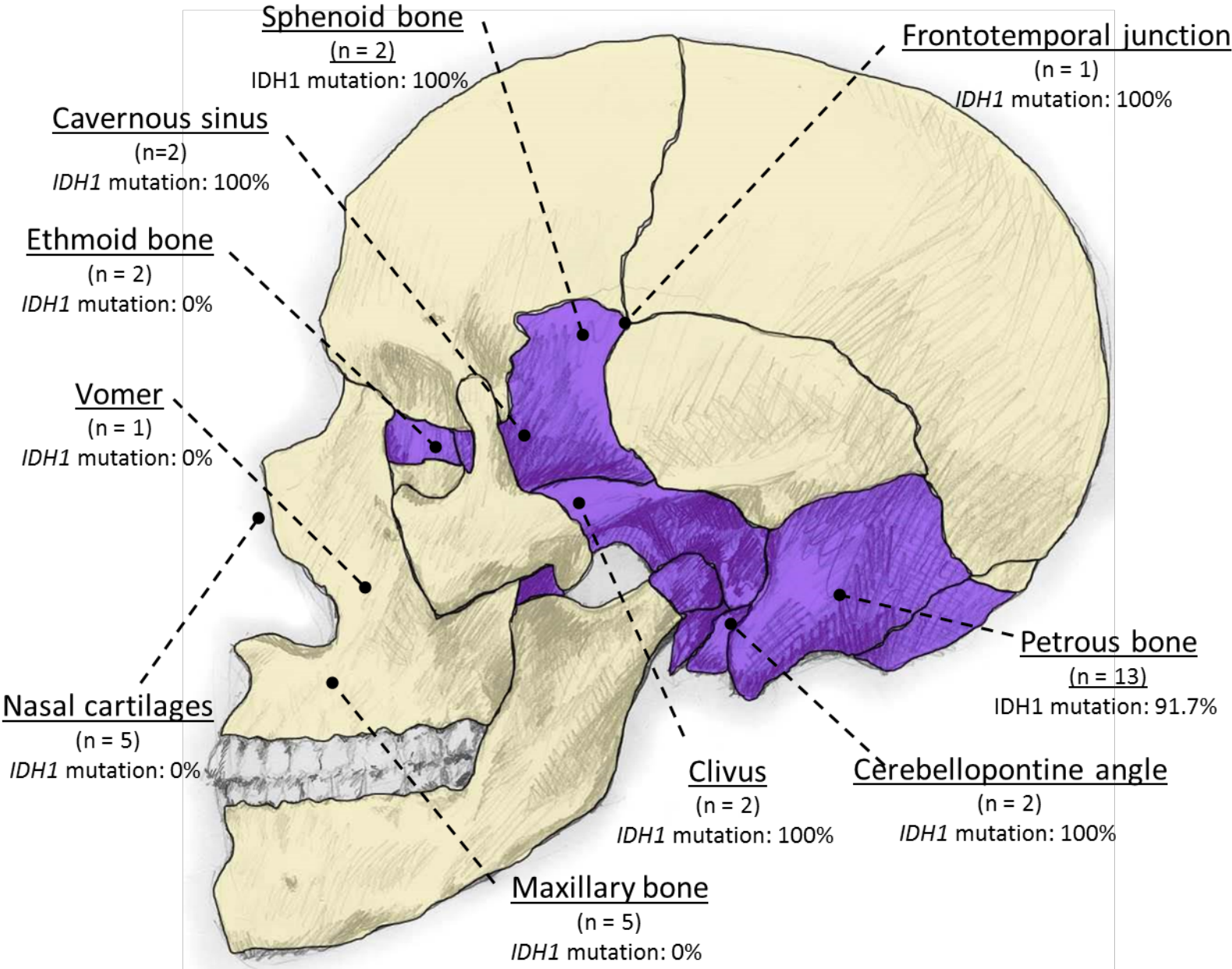


Table 1. PCR primers used for *IDH1* and *IDH2* mutations detection by pyrosequencing.
IDH : isocitrate dehydrogenase

<i>Primer name</i>	<i>Sequence</i>
IDH1-PY-F1	5'-TGGATGGGTAAAACCTATCATCA-3'
IDH1-PY-R1B	5'-Biotin-GACTTACTTGACCCCATAAGCA-3'
IDH1-PY-S1	5'-TGATCCCCATAAGCAT-3'

<i>Primer name</i>	<i>Sequence</i>
IDH2-PY-F2	5'-AACATCCCACGCCTAGTCCCT-3'
IDH2-PY-R2B	5'-Biotin-CTCTCCACCCTGGCCTACCT-3'
IDH2-PY-S2	5'-AGCCCATCACCATTG-3'

Table 2. Clinicopathological characteristics of the laryngeal and tracheal chondrosarcomas.

M: men; W: women; NOS : not otherwise specified

	n (%)
<i>Number of cases</i>	47
<i>Sex</i>	
Men	27 (57.4%)
Women	19 (40.4%)
NOS	1 (2.1%)
<i>sex ratio (M/W)</i>	1.42
<i>Mean age (years), [range]</i>	64.8 [31-90]
<i>Tumor location</i>	
Laryngeal	
Larynx, NOS	21 (44.7%)
Cricoid cartilage	15 (31.9%)
Thyroid cartilage	3 (6.4%)
Epiglottis	1 (2.1%)
Trachea	7 (14.9%)
<i>Histological grade</i>	
Available	46 (97.9%)
Grade 1	27 (58.7%)
Grade 2	18 (39.1%)
Grade 3	1 (2.2%)

Table 3. Clinical and histological characteristics of the craniofacial chondrosarcomas, including tumors of the skull base and facial skeleton.
M: men; W: women; NOS: not otherwise specified

	Skull base n (%)		Facial skeleton n (%)
<i>Number of cases</i>	30		11
<i>Sex</i>			
Men	10 (33.3%)		8 (72.7%)
Women	20 (66.7%)		3 (27.3%)
<i>Sex ratio (M/W)</i>	0.5		2,67
<i>Mean age (years), [range]</i>	45.1 [17-81]		44.1 (16-89)
<i>Tumor location</i>			
Skull base, NOS	6 (20.0%)	Maxillary bone	5 (45.5%)
Petrous bone	13 (43.3%)	Vomer	1 (9.1%)
Ethmoid bone	2 (6.7%)	Nasal septum	5 45.5%
Cerebellopontine angle	2 (6.7%)		
Clivus	2 (6.7%)		
Cavernous sinus	2 (6.7%)		
Sphenoid bone, NOS	2 (6.7%)		
Fronto-temporal junction	1 (3.3%)		
<i>Histological grade</i>			
Available	27 (90.0%)		10 (90.9 %)
Grade 1	5 (18.5%)		5 (50%)
Grade 2	21 (77.8%)		5 (50%)
Grade 3	1 (3.7%)		0 (0%)

Table 4. Chondrosarcomas involving the laryngotracheal tract

G1 : grade 1 ; G2 : grade 2 ; G3 : grade 3 ; NI : not interpretable ; NOS : not otherwise specified.

Case	Tumor location	Tumor grade	IDH mutation status
1	Trachea	G1	IDH wild-type
2	Larynx, NOS	G1	IDH wild-type
3	Thyroid cartilage	G1	IDH wild-type
4	Trachea	G1	IDH1 (R132G)
5	Trachea	G1	IDH wild-type
6	Trachea	G1	IDH wild-type
7	Larynx, NOS	G1	IDH wild-type
8	Larynx, NOS	G1	IDH wild-type
9	Larynx, NOS	G2	IDH1 (R132C)
10	Thyroid cartilage	NOS	IDH wild-type
11	Larynx, NOS	G2	IDH wild-type
12	Larynx, NOS	G1	IDH wild-type
13	Larynx, NOS	G1	IDH wild-type
14	Larynx, NOS	G1	NI
15	Larynx, NOS	G1	IDH wild-type
16	Larynx, NOS	G1	NI
17	Cricoid cartilage	G1	IDH wild-type
18	Cricoid cartilage	G1	IDH wild-type
19	Cricoid cartilage	G2	IDH wild-type
20	Cricoid cartilage	G2	IDH wild-type
21	Cricoid cartilage	G2	IDH wild-type
22	Thyroid cartilage	G1	IDH wild-type
23	Cricoid cartilage	G1	IDH wild-type
24	Larynx, NOS	G1	IDH wild-type
25	Cricoid cartilage	G2	IDH wild-type
26	Larynx, NOS	G2	IDH wild-type
27	Cricoid cartilage	G1	NI
28	Larynx, NOS	G1	NI
29	Larynx, NOS	G1	NI
30	Epiglottis	G2	IDH wild-type
31	Larynx, NOS	G2	IDH wild-type
32	Trachea	G3	NI
33	Larynx, NOS	G2	NI
34	Cricoid cartilage	G1	NI
35	Cricoid cartilage	G1	NI
36	Larynx, NOS	G1	NI
37	Larynx, NOS	G2	NI
38	Larynx, NOS	G1	IDH wild-type
39	Cricoid cartilage	G2	IDH1 (R132C)
40	Cricoid cartilage	G2	NI
41	Trachea	G2	IDH wild-type
42	Larynx, NOS	G2	IDH wild-type
43	Cricoid cartilage	G2	NI
44	Cricoid cartilage	G2	IDH wild-type
45	Larynx, NOS	G1	IDH wild-type
46	Cricoid cartilage	G1	IDH1 (R132C)
47	Trachea	G2	IDH wild-type

Table 5. Chondrosarcomas involving the base of the skull and the facial skeleton.

G1 : grade 1 ; G2 : grade 2 ; G3 : grade 3; NI : not interpretable ; NOS : not otherwise specified.

Case	Tumor location	Tumor grade	<i>IDH</i> mutation status
1	Petrous bone	G2	<i>IDH1</i> (R132C)
2	Skull base, NOS	G2	<i>IDH1</i> (R132C)
3	Skull base, NOS	NOS	<i>IDH1</i> (R132C)
4	Skull base, NOS	G2	<i>IDH1</i> (R132C)
5	Petrous bone	G1	<i>IDH1</i> (R132C)
6	Cerebellopontine angle	G1	<i>IDH1</i> (R132G)
7	Ethmoid bone	NOS	<i>IDH</i> wild-type
8	Cerebellopontine angle	NOS	<i>IDH1</i> (R132G)
9	Petrous bone	G1	<i>IDH1</i> (R132L)
10	Petrous bone	G2	<i>IDH</i> wild-type
11	Frontotemporal junction	G2	<i>IDH1</i> (R132C)
12	Petrous bone	G2	<i>IDH1</i> (R132C)
13	Clivus	G2	<i>IDH1</i> (R132C)
14	Petrous bone	G2	<i>IDH1</i> (R132C)
15	Petrous bone	G2	<i>IDH1</i> (R132C)
16	Petrous bone	G2	<i>IDH1</i> (R132C)
17	Petrous bone	G2	<i>IDH1</i> (R132C)
18	Skull base, NOS	G2	<i>IDH1</i> (R132L)
19	Petrous bone	G2	<i>IDH1</i> (R132C)
20	Skull base, NOS	G2	<i>IDH</i> wild-type
21	Petrous bone	G2	NI
22	Sphenoid bone	G2	NI
23	Petrous bone	G1	<i>IDH1</i> (R132G)
24	Cavernous sinus	G2	<i>IDH1</i> (R132C)
25	Cavernous sinus	G2	<i>IDH1</i> (R132G)
26	Skull base, NOS	G1	<i>IDH1</i> (R132H)
27	Clivus	G2	<i>IDH1</i> (R132S)
28	Ethmoid bone	G3	<i>IDH</i> wild-type
29	Petrous bone	G2	<i>IDH1</i> (R132L)
30	Sphenoid bone	G2	<i>IDH1</i> (R132C)
31	Nasal septum	G1	<i>IDH</i> wild-type
32	Nasal septum	G2	<i>IDH</i> wild-type
33	Nasal septum	G1	<i>IDH</i> wild-type
34	Nasal septum	G2	<i>IDH</i> wild-type
35	Nasal septum	G1	NI
36	Maxillary bone	G2	<i>IDH</i> wild-type
37	Maxillary bone	NOS	NI
38	Maxillary bone	G2	<i>IDH</i> wild-type
39	Maxillary sinus	G2	<i>IDH</i> wild-type
40	Vomer	G1	<i>IDH</i> wild-type
41	Maxillary bone	G1	<i>IDH</i> wild-type